Thermodynamic properties of $S=2$ antiferromagnetic Heisenberg chains

Shoji Yamamoto
Department of Physics, Faculty of Science, Osaka University, Toyonaka, Osaka 560, Japan
(Received 14 September 1995)

Thermodynamic properties of $S=2$ antiferromagnetic Heisenberg chains are studied not only under the periodic boundary condition but also under the open one employing a quantum Monte Carlo method. Temperature and size dependences of the energy, the specific heat, and the magnetic susceptibility are calculated and edge effects on them are investigated in detail. The specific heat shows a well-pronounced Schottky anomaly but the maximum is located at a temperature much larger than the Haldane gap of the system. As temperature goes to zero, the magnetic susceptibility vanishes for the periodic chains, while it diverges for the open chains. The edge contribution in the open-chain susceptibility is attributed to the two $S=1$ effective spins localized at the chain ends at low temperatures, while to an $S=2$ free spin at high temperatures. This is a visualization of a quantum-classical crossover and an evidence that the present model is a Haldane system. High-temperature behaviors of the thermodynamic quantities are also discussed with the help of a series-expansion method.

I. INTRODUCTION

Haldane's conjecture[1] caused integer-S linear-chain Heisenberg antiferromagnets to catch a great deal of attention. The so-called Haldane gap immediately above the ground state is now widely believed to exist and a precise estimate of the $S=1$ Haldane gap[2,3] has been recently given. Besides the gap, various nontrivial ground-state properties of the Haldane antiferromagnets have been revealed so far, such as the exponential decay of the spin correlation function,[2–6] the effective spins localized at chain ends,[7,8] and the hidden antiferromagnetic order.[9] It should be also noted that an exactly solvable model[10] introduced by Affleck, Kennedy, Lieb, and Tasaki has played an important role in understanding the underlying physical mechanism of these phenomena.

The experimental study has been successfully carried out especially since the synthesis of an $S=1$ quasi-one-dimensional antiferromagnet, $Ni(C_2H_8N_2)_2NO_2ClO_4$,[11] which is abbreviated as NENP. Renard *et al.*[11] demonstrated that magnetic susceptibility and inelastic neutron scattering experiments on NENP are well explained by the existence of an energy gap between the ground state and the first excited state. Katsumata *et al.*[12] further performed magnetization measurements on NENP and confirmed that NENP is actually a Haldane-gap material. Since then, a variety of $S=1$ linear-chain antiferromagnets[13–15] have been successfully synthesized and they have in general supported Haldane's conjecture. Motivated by these stimulative experiments, the present author and Miyashita have recently studied on thermodynamic[16,17] and magnetic[18] properties of $S=1$ antiferromagnetic Heisenberg chains using a quantum Monte Carlo method. Few theoretical studies on finite-temperature properties of the Haldane antiferromagnet had been well presented until these investigations. Of course, before Haldane's conjecture, there had already been several pioneering works[19–21] on thermodynamic quantities of the integer-S chains, which employed a numerical diagonalization method. However, in these works, any remarkable property peculiar to the Haldane system was not yet mentioned. It was also unfortunate in the works that the calculations were restricted to rather short chains. A few more fine works[22,23] on thermal properties of the $S=1$ chains were presented during the last decade. Betsuyaku and Yokota[22] calculated temperature and anisotropy dependences of the energy and the specific heat using a quantum transfer-matrix method. However, their work seems to have aimed at demonstrating usefulness of the method rather than inquiring into the Haldane problem. While Narayanan and Singh[23] investigated the specific heat in the bulk by means of a cluster expansion method in lattice gauge theories, boundary condition and size dependences of the quantity were not explicitly discussed. In such above-mentioned circumstances, our works[8,16–18] laid special emphasis on the open-chain properties and treated the Haldane problem in connection with the edge effects. The edge state,[7,8] as well as the Haldane gap, is a fascinating subject not only theoretically but also experimentally in that it is a macroscopic consequence of quantum cooperative phenomena. Recent experiments[24–30] are actually showing an interest in the doped materials aiming to observe the edge effects.

In order to obtain an essential understanding of the Haldane problem, it is necessary to study the $S=2$ systems. However, in comparison with a variety of $S=1$ studies, the $S=2$ systems have been less discussed so far partly because of the large degree of freedom. Therefore, it is great encouragement to the $S=2$ study to have been demonstrated[31,32] that the valence-bond approach[10] is still successful in the $S\geqslant 2$ cases. There are, on the other hand, recent numerical attempts[33–39] to treat the pure $S=2$ Heisenberg chains. Although the Haldane gap is expected to decrease rapidly as S increases, several authors[35–39] have given pioneering estimates of the $S=2$ Haldane gap, which are still somewhat different from one another. All the recent $S=2$ works are stimulative, whereas they have not yet discussed the finite-temperature properties. Thus we here carry out Monte Carlo calculations of thermodynamic properties of $S=2$ antiferromagnetic Heisenberg chains. We investigate temperature dependences of the energy, the specific heat, and the (zero-field) magnetic susceptibility not only for the periodic chains

but also for the open ones. The present study is also motivated by recent admirable experimental attempts[40,41] to observe magnetic properties of the $S=2$ linear-chain Heisenberg antiferromagnet and possibly discuss the $S=2$ Haldane phenomena. It is unfortunate that all the existing $S=2$ materials[40,41] exhibit the three-dimensional antiferromagnetic order at temperatures much larger than the Haldane gap predicted theoretically.[35–39] We hope that $S=2$ Haldane antiferromagnets will be successfully synthesized in the future and the present study can be of some help to analysis of the experimental results on them.

In Sec. II, we describe in detail the Monte Carlo procedure. Obtaining numerically reliable results with feasible Monte Carlo steps in the $S=2$ cases is not so trivial as that in the smaller-S cases due to the large degree of freedom. The present numerical accuracy is checked employing a quantum transfer-matrix method and also in comparison with exact diagonalization results. In Sec. III, we present the results and discuss them. Section IV is devoted to summary.

II. METHOD

We treat the $S=2$ antiferromagnetic Heisenberg chains described by the Hamiltonian

$$\mathscr{H}=\sum_{i=1}^{L} J_i \mathbf{S}_i\cdot\mathbf{S}_{i+1}-g\mu_B H\sum_{i=1}^{L} S_i^z, \tag{2.1}$$

where g is the g factor of the spin, μ_B the Bohr magneton, L the number of spins, and $\mathbf{S}_{L+1}=\mathbf{S}_1$. The exchange interaction J_i is taken according to the boundary condition as

$$J_1=J_2=\cdots=J_L=J \quad \text{for the periodic chains,} \tag{2.2a}$$

$$J_1=J_2=\cdots=J_{L-1}=J,\ J_L=0 \quad \text{for the open chains.} \tag{2.2b}$$

The partition function $Z=\mathrm{Tr}[e^{-\beta\mathscr{H}}]$ is approximately decomposed as[42]

$$Z\simeq \mathrm{Tr}\left[\left(\prod_{i=1,3,\ldots} e^{-\beta h_i/n}\prod_{i=2,4,\ldots} e^{-\beta h_i/n}\right)^n\right], \tag{2.3}$$

where n is a Trotter number, $\beta=(k_BT)^{-1}$ with the Boltzmann constant k_B, and

$$h_i=J_i\mathbf{S}_i\cdot\mathbf{S}_{i+1}-\frac{g\mu_B H}{2}(S_i^z+S_{i+1}^z) \tag{2.4}$$

is the local Hamiltonian. Using the local Boltzmann factor [Fig. 1(a)],

$$\rho_i^{(m)}=\langle S_i^{(m)},S_{i+1}^{(m)}|e^{-\beta h_i/n}|S_i^{(m+1)},S_{i+1}^{(m+1)}\rangle, \tag{2.5}$$

which is represented as a square matrix of 25×25 size, Eq. (2.3) is rewritten as

$$Z\simeq\sum_{\{S_i^{(m)}\}}\prod_{l=1}^{n}\left(\prod_{i=1,3,\ldots}\rho_i^{(2l-1)}\prod_{i=2,4,\ldots}\rho_i^{(2l)}\right), \tag{2.6}$$

where $S_i^{(2l-1)}$ and $S_i^{(2l)}$ are Ising spins at the ith site on the lth Trotter layer. Here, $S_i^{(2n+1)}=S_i^{(1)}$ and $S_i^{(m)}$ takes 0, ±1, and ±2. $\Sigma_{\{S_i^{(m)}\}}$ denotes the summation over all the configurations of the Ising spins on the transformed $(1+1)$-dimensional checkerboard,[43] which is here evaluated through an importance sampling.[44]

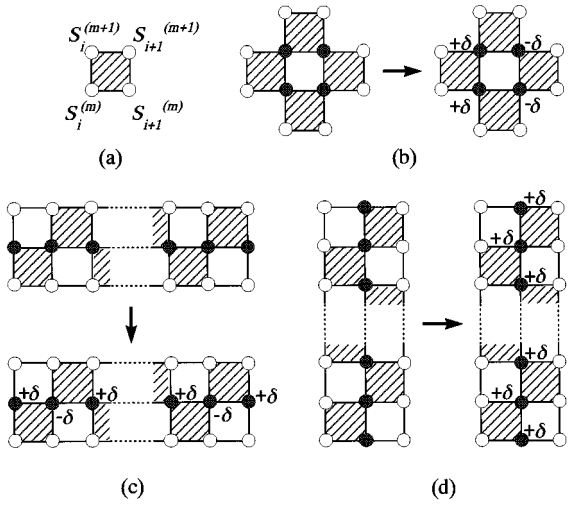

FIG. 1. Various types of Monte Carlo flips on the transformed two-dimensional Ising system, where the circles denote the Ising spins, the hatched plaquettes the local Boltzmann factors, and the shaded circles the spins to be updated. (a) Plaquette with the four-body interaction, where $S_i^{(m)}$ takes 0, ±1, and ±2. Here i and m are the indices representing a site and a Trotter layer, respectively: $i=1,2,\ldots,L$; $m=1,2,\ldots,2n$. (b) Local flip which updates a set of four spins as $\{S_i^{(m+1)},S_{i+1}^{(m+1)},S_i^{(m+2)},S_{i+1}^{(m+2)}\}\rightarrow\{S_i^{(m+1)}+\delta,S_{i+1}^{(m+1)}-\delta,\ S_i^{(m+2)}+\delta,S_{i+1}^{(m+2)}-\delta\}$, where δ takes 0, ±1, and ±2. (c) Global flip along the chain direction which updates a set of L spins as $\{S_1^{(m)},S_2^{(m)},\ldots,S_L^{(m)}\}\rightarrow\{S_1^{(m)}+\delta,S_2^{(m)}-\delta,\ldots,S_L^{(m)}-(-1)^L\delta\}$, where δ takes 0, ±1, and ±2. (d) Global flip along the Trotter direction which updates a set of $2n$ spins as $\{S_i^{(1)},S_i^{(2)},\ldots,S_i^{(2n)}\}\rightarrow\{S_i^{(1)}+\delta,S_i^{(2)}+\delta,\ldots,S_i^{(2n)}+\delta\}$, where δ takes 0, ±1, and ±2. The local flips (b) and the global flips (c) are done keeping the total magnetization of the chain constant. The flips (c) change the winding number of the spin configuration and are therefore necessary only for periodic chains. The total magnetization of the chain fluctuates through the global flips (d). The flips of types (b) and (c) represent quantum fluctuations, while the flips of type (d) thermal fluctuations.

Now let me describe the actual Monte Carlo procedure to update the spin configuration. The local flips [Fig. 1(b)] are the most fundamental and are carried out keeping the total magnetization of the chain constant. The global flips along the chain direction [Fig. 1(c)], which also keep the total magnetization constant, change the winding number[43] of the spin configuration and are thus necessary only for periodic chains. Although the global flips of this type should be in principle taken into account, they are sometimes neglected due to their small effect. However, we have confirmed that, in the present case, an improvement of the Monte Carlo estimate owing to this type of global flips is generally beyond the numerical uncertainty. Therefore, we have taken them into the calculational procedure. It seems that this type of global flip becomes more effective as S increases. In contrast to the above-mentioned flips, the global flips along the Trotter direction [Fig. 1(d)] are carried out to let the total magnetiza-

TABLE I. Monte Carlo estimates and exact transfer-matrix calculations of the energy of the 4×4 Ising system at various temperatures, where PBC and OBC mean the periodic and open boundary conditions, respectively.

	PBC		OBC	
k_BT/J	Monte Carlo	Exact	Monte Carlo	Exact
0.1	−23.99605 (0.00244)	−23.99946	−17.97939 (0.00158)	−17.97937
0.2	−23.87768 (0.00346)	−23.91735	−17.69235 (0.00605)	−17.69099
0.3	−23.47065 (0.00664)	−23.55246	−17.18408 (0.00848)	−17.18291
0.4	−22.93137 (0.00834)	−23.02476	−16.70855 (0.00838)	−16.70624
0.5	−22.41956 (0.01000)	−22.51492	−16.29418 (0.01035)	−16.29322
0.6	−21.95668 (0.00944)	−22.05656	−15.92750 (0.00946)	−15.92750
0.8	−21.14744 (0.01294)	−21.25486	−15.29670 (0.01399)	−15.29197
1.0	−20.44814 (0.01902)	−20.55565	−14.72980 (0.01574)	−14.72834

tion change. All the flips are schematically shown in Fig. 1, where δ takes 0, ±1, and ±2. It is not necessary for the ergodic distribution that δ takes ±2. We also admit that more candidates for a new configuration in the flipping procedure make the numerical argorithm more complicated. Nevertheless, we have provided δ with the five values because we have found out that the simulation with $\delta=0,\pm1$ sometimes gives initial-configuration-dependent results. This is a serious problem which may be left unnoticed from an ergodic point of view but is essential in the actual calculations. We cannot be too careful with the large degree of freedom.

In order to check the numerical accuracy in the present method, we compare, in Table I, the Monte Carlo estimates and the exact values for the energy (in the unit of J) of the 4×4 ($L=4$ and $n=2$) Ising system at various temperatures, where 3×10^4 and 2×10^5 Monte Carlo steps have been spent on the initial thermalization and the Monte Carlo sampling, respectively, at each temperature, and the numerals in parentheses are the statistical uncertainties in the sampling. Here the exact energies have been calculated by means of a quantum transfer-matrix method,[22,45,46] that is, by tracing out all the configurations of the system. We find that the precision of the Monte Carlo data is, at least, almost three digits, namely, there is, at worst, small uncertainty in the first decimal place. Under the open boundary condition, the differences between the Monte Carlo estimates and the exact values are all within the statistical uncertainties, while under the periodic boundary condition, they are generally beyond those. The small but nontrivial deviations under the periodic boundary condition result from the winding-number problem and are therefore expected to decrease with increase of the system size. On the other hand, the statistical errors are generally enhanced with increase of the Trotter number, because the acceptance ratio of the global flips along the Trotter direction is strongly reduced for large Trotter numbers. Thus, in the actual calculations which have been carried out for large L's and n's, the dominant numerical uncertainties in the Monte Carlo data generally come from the statistical errors. We list in Table II sets of the Trotter numbers used at various temperatures, together with the Monte Carlo steps spent for each Trotter number. With decrease of temperature, larger Trotter numbers are taken not to freeze the spin configuration and more Monte Carlo steps are spent on equilibrating the system.

We have to extrapolate a set of Monte Carlo data for finite Trotter numbers into the $n\to\infty$ limit to obtain a final result. The n dependence is extrapolated by the least squares method with a formula[45]

$$A(n)=A_\infty+\frac{A_1}{n^2}+\frac{A_2}{n^4}. \tag{2.7}$$

We show in Fig. 2 how the Monte Carlo data for the energy are extrapolated, where $L=8$ and $k_BT/J=0.02$. Since the temperature is low enough to represent the ground-state properties, the $n\to\infty$ extrapolated values are expected to coincide with the exact-diagonalization results[47] for the ground-state energy. The open-chain result is in excellent agreement with the exact one, while the periodic-chain result, as expected, shows a slight deviation from the exact

TABLE II. Sets of the Trotter numbers used and the Monte Carlo steps (MCS) spent for each Trotter number at various temperatures.

k_BT/J	n	MCS
0.08 | 0.11	12, 16, 24, 32	6×10^5
0.13	10, 14, 20, 28	5×10^5
0.15	8, 12, 16, 24	5×10^5
0.20	6, 8, 12, 16	5×10^5
0.30 | 0.50	4, 6, 8, 12	4×10^5
0.60 | 1.00	2, 4, 6, 8	3×10^5
1.20 | 10.00	2, 4, 6, 8	2×10^5

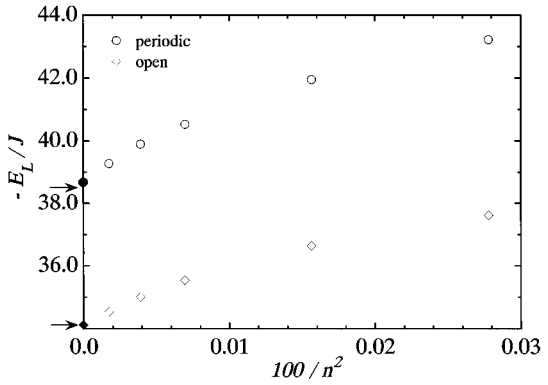

FIG. 2. Trotter number dependences of the Monte Carlo data for the energy in the periodic (○) and open (◇) chains with $L=8$ at $k_BT/J=0.02$. The statistical uncertainties in the data are smaller than their symbols. ● and ◆ denote the $n\to\infty$ values obtained by extrapolating the data ○ and ◇, respectively. The arrows indicate the ground-state energies (Ref. 47) of the $L=8$ periodic and open chains, which were calculated by means of a numerically exact diagonalization method.

one. However, even the periodic-chain result has almost three-digits reliability and its deviation almost disappears into the statistical uncertainty.

Now we may say that the numerical accuracy of the final results is between three and two digits at low temperatures and between four and three digits at high temperatures. The worst accuracy is found in the low-temperature calculations of the specific heat C which has been directly evaluated through a formula[48]

$$C=\frac{1}{k_BT^2}(\langle Q^2\rangle-\langle Q\rangle^2+\langle Q'\rangle), \tag{2.8}$$

where

$$Q=\sum_{i,m}\left[\frac{1}{\rho_i^{(m)}}\frac{\partial\rho_i^{(m)}}{\partial\beta}\right],$$
$$Q'=\sum_{i,m}\left[\frac{1}{\rho_i^{(m)}}\frac{\partial^2\rho_i^{(m)}}{\partial\beta^2}-\left(\frac{1}{\rho_i^{(m)}}\frac{\partial\rho_i^{(m)}}{\partial\beta}\right)^2\right], \tag{2.9}$$

and $\langle A\rangle$ denotes the thermal average of A at a given temperature. On the other hand, the data for the energy E which have been obtained through a formula[48]

$$E=-\langle Q\rangle, \tag{2.10}$$

generally have higher accuracy than those for the specific heat. Therefore, the specific heat at low temperatures ($k_BT/J\leqslant 0.6$) has been calculated by numerically differentiating the energy with respect to temperature, though the accuracy still did not reach three digits. The magnetic susceptibility χ has been calculated through a formula

$$\chi=\frac{g^2\mu_B^2}{k_BT}(\langle M'\rangle-\langle M\rangle^2), \tag{2.11}$$

where

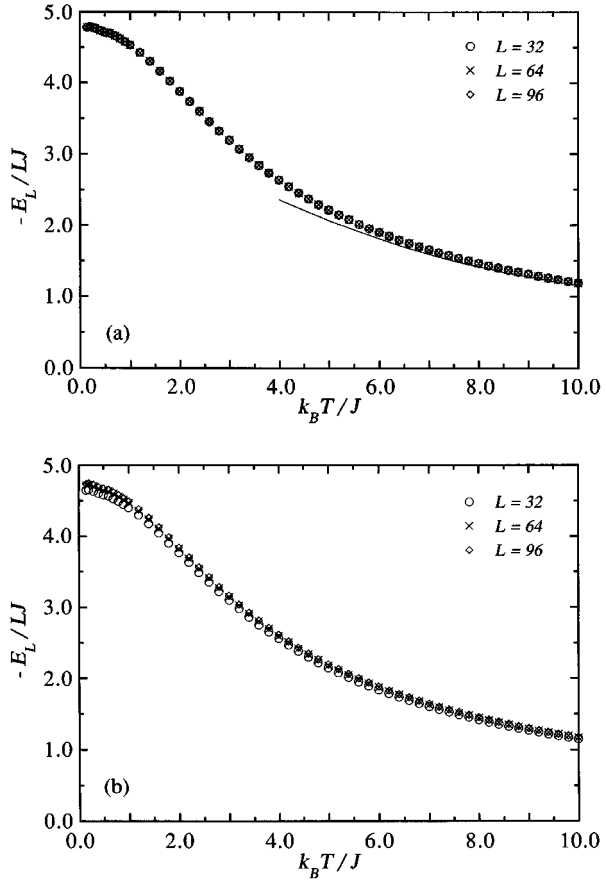

FIG. 3. Temperature dependences of the energy E_L per spin in the periodic (a) and open (b) chains with various lengths L. The solid line represents a high-temperature series-expansion result for the periodic chain within the up-to-$(\beta J)^3$ approximation.

$$M=\frac{1}{2n}\sum_{i,m}S_i^{(m)},$$
$$M'=\frac{1}{2n}\sum_m\left(\sum_i S_i^{(m)}\right)^2. \tag{2.12}$$

III. RESULTS AND DISCUSSION

A. Energy

We show in Fig. 3 temperature dependences of the energy per spin in the periodic [Fig. 3(a)] and open [Fig. 3(b)] chains. Though a weak size dependence is observed for the open chains, both the periodic and open chains show almost the same behavior at $L=96$, that may be regarded as the bulk property. A stationary point at $k_BT/J\simeq 2$ suggests the existence of the Schottky anomaly in temperature dependences of the specific heat. Let us confirm the high-temperature behavior of the energy by means of a series-expansion method. Carefully treating the edge effect, we find that

$$E_L=\frac{\mathrm{Tr}[\mathscr{H}e^{-\beta\mathscr{H}}]}{\mathrm{Tr}[e^{-\beta\mathscr{H}}]}=\begin{cases}E_\infty L\equiv E_L^{\mathrm{per}} & \text{for the periodic chains,}\\ E_\infty L+E_0\equiv E_L^{\mathrm{open}} & \text{for the open chains,}\end{cases} \tag{3.1}$$

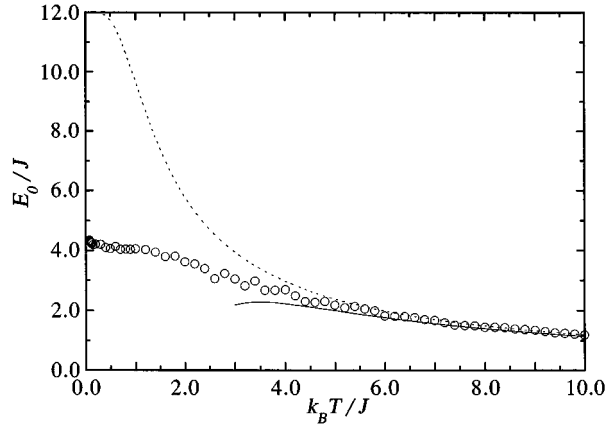

FIG. 4. Temperature dependence of the finite-size correction in the energy, $E_0=E_L^{\rm open}-E_L^{\rm per}$, obtained from the $L=96$ data. The solid line represents a high-temperature series-expansion result within the up-to-$(\beta J)^3$ approximation. The dashed line represents the temperature dependence of the energy of an antiferromagnetically coupled $S=2$ classical spin pair.

where

$$E_\infty=J\left(-12\beta J+\frac{204}{5}(\beta J)^3\right)+O\left((\beta J)^5\right), \quad (3.2a)$$

$$E_0=J\left(12\beta J-\frac{244}{5}(\beta J)^3\right)+O\left((\beta J)^5\right). \quad (3.2b)$$

We have plotted in Fig. 3(a) the expression (3.2a), which is in good agreement with the numerical data especially at $k_BT/J\gtrsim 6=[S(S+1)]_{S=2}$. Figure 4 shows that the expression (3.2b) also well fits the numerical result for the finite-size correction $E_0=E_L^{\rm open}-E_L^{\rm per}$ at high temperatures. We have confirmed that all the data for $L=32$, 64, 96 give almost the same results for E_0. The dashed line in Fig. 4 represents the temperature dependence of the energy of an antiferromagnetically coupled $S=2$ classical spin pair,

$$E=3J\times\frac{16\ \sinh[4\beta J]+16\ \sinh[2\beta J]+4\ \sinh[\beta J]}{4\ \cosh[4\beta J]+8\ \cosh[2\beta J]+4\ \cosh[\beta J]+9}, \quad (3.3)$$

which well explains the numerical data at $k_BT/J\gtrsim 4$. We find that at high temperatures, the system can be regarded as a group of almost free spins which are weakly coupled to one another. On the other hand, the edge effects at low temperatures should be understood in connection with the edge states which are composed of quantum mechanically correlated spins, as will be shown in Sec. III C.

B. Specific heat

We show in Fig. 5 temperature dependences of the specific heat per spin in the periodic [Fig. 5(a)] and open [Fig. 5(b)] chains. The temperature dependence at $L=96$ is in good agreement with the $L\to\infty$ result[20] obtained by extrapolating the numerical-diagonalization data for $L\leqslant 5$, except for small deviations at low temperatures. There exists a well-pronounced maximum (Schottky anomaly) due to the existence of an energy gap. However, the temperature dependence should not be simply attributed to the Haldane gap of the system, which is probably smaller than $0.1J$,[35–39] because the maximum is located at $k_BT/J\simeq 2$. While the open chains show a weak size dependence as expected, it is significant around the Schottky anomaly rather than at low temperatures. An asymptotic high-temperature behavior of the specific heat is straightforwardly obtained from Eqs. (3.1) and (3.2) as

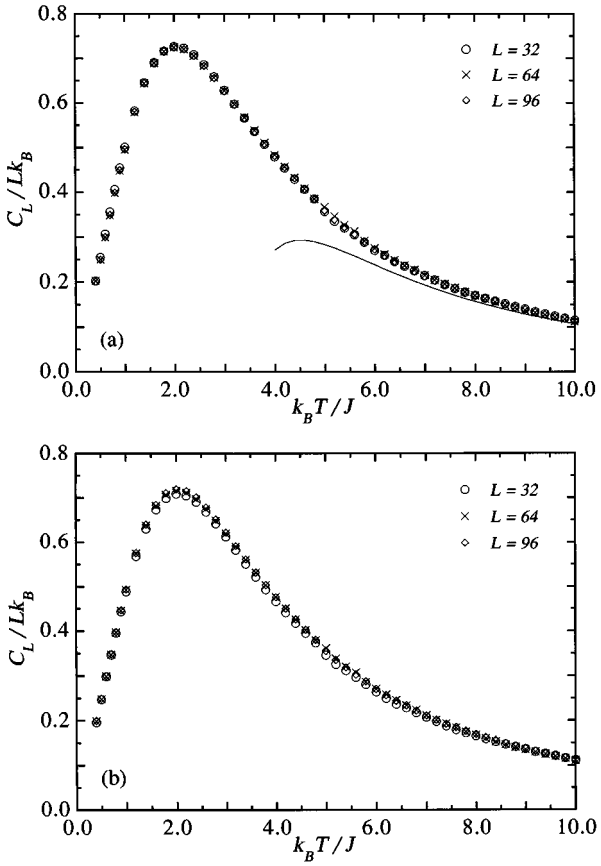

FIG. 5. Temperature dependences of the specific heat C_L per spin in the periodic (a) and open (b) chains with various lengths L. The solid line represents a high-temperature series-expansion result for the periodic chain within the up-to-$(\beta J)^4$ approximation.

$$C_L=\begin{cases} C_\infty L\equiv C_L^{\rm per} & \text{for the periodic chains,} \\ C_\infty L+C_0\equiv C_L^{\rm open} & \text{for the open chains,} \end{cases} \quad (3.4)$$

where

$$C_\infty=k_B\left(12(\beta J)^2-\frac{612}{5}(\beta J)^4\right)+O\left((\beta J)^6\right), \quad (3.5a)$$

$$C_0=k_B\left(-12(\beta J)^2+\frac{732}{5}(\beta J)^4\right)+O\left((\beta J)^6\right). \quad (3.5b)$$

The expression (3.5a) has been also shown in Fig. 5(a).

Due to the Haldane gap, it is expected that the specific heat vanishes exponentially as $T\to 0$. Unfortunately, however, we were unable to calculate the specific heat success-

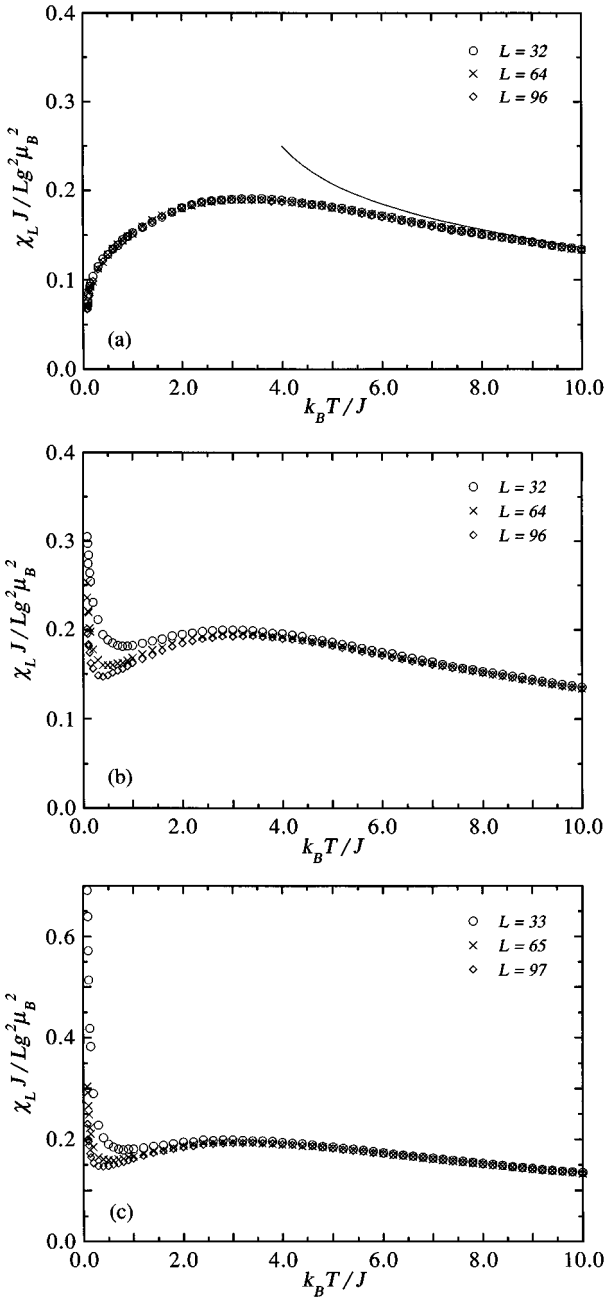

FIG. 6. Temperature dependences of the magnetic susceptibility χ_L per spin in the periodic (a) and open [(b) and (c)] chains with various lengths L. The solid line represents a high-temperature series-expansion result for the periodic chain within the up-to-$(\beta J)^3$ approximation.

fully at such low temperatures. On the other hand, it is interesting that a T-linear behavior exists over a finite interval. The behavior is, within 10% deviation, consistent with Kubo's antiferromagnetic spin-wave theory result[49]

$$\frac{C_L}{Lk_B}=\frac{\pi k_BT}{3JS}. \tag{3.6}$$

There is a variational approach[50] concluding that a T-linear behavior of the specific heat may also exist over a certain interval for finite-gap systems. It seems that formula (3.6) holds better for large spins than for small ones.[20] There are also recent reports[35,39] that the elementary excitation spectrum of the present system is, within 10% deviation, consistent with Anderson's spin-wave theory result[51] except for the qualitative difference at the boundaries and center of the Brillouin zone. While we have to keep it in mind that Anderson's approach is a semiclassical one,[51] we may say that the spin-wave picture generally comes to hold better as S increases.

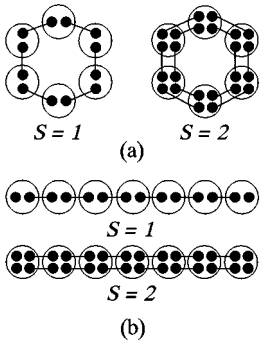

FIG. 7. Schematic representations of the VBS state on a periodic chain (a) and a VBS-like state on an open chain (b) in the cases of $S=1$ and $S=2$, where the symbol ● and the segment denote a spin 1/2 and a singlet pair, respectively. The circle represents an operation of constructing a spin S by symmetrizing the $2S$ spin 1/2's inside.

C. Magnetic susceptibility

We show in Fig. 6 temperature dependences of the magnetic susceptibility per spin in the even-length periodic chains [Fig. 6(a)], the even-length open chains [Fig. 6(b)], and the odd-length open chains [Fig. 6(c)]. As $T\rightarrow 0$, χ_L vanishes for the periodic chains, while diverges for the open chains. We note that the divergence in the present system is essentially different from one in the half-odd-integer-S

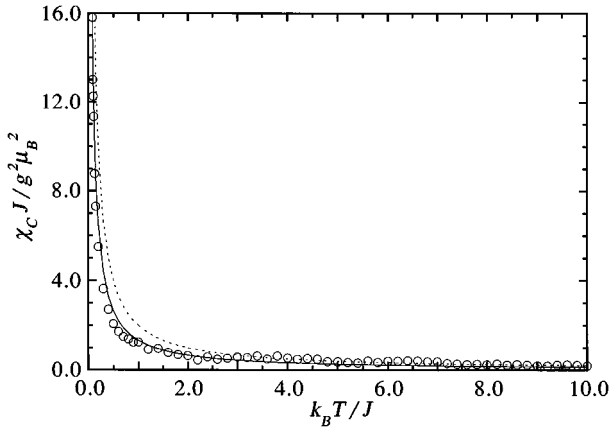

FIG. 8. Temperature dependence of the edge contribution in the magnetic susceptibility, $\chi_C=\chi_{L+1}^{\rm open}-\chi_L^{\rm per}$, obtained from the $L=96$ data. The solid and dashed lines represent the curves, $\chi_C J/g^2\mu_B^2=(4/3)(k_BT/J)^{-1}$ and $\chi_C J/g^2\mu_B^2=2(k_BT/J)^{-1}$, respectively, which are expected for two isotropic spins of $S=1$ and for an isotropic spin of $S=2$.

chains,[52] where as $T\to 0$, regardless of the boundary condition, χ_L vanishes for the even-length chains, while it diverges for the odd-length chains. It is the quasi-nine-fold degeneracy[36] of the open-chain ground states that bears the divergence in Fig. 6, as will be made clear in the following. The $(S+1)^2$-fold degenerate ground states of an open chain are a remarkable property probably common throughout the Haldane systems[10,53,54] and have been actually detected for the $S=1$ (Refs. 7, 8, and 55) and $S=2$ (Ref. 36) Heisenberg Hamiltonians. It has been also pointed out[10,55] that the magnetic ground states of the same origin is further found for a variety of models with Haldane gap. Thus the low-temperature behavior of the susceptibility shown here is evidence that the present system is in a massive phase of Haldane type.

The mechanism of this phenomenon is well understood by means of a valence-bond approach[10,53] schematically shown in Fig. 7. Since the so-called valence-bond-solid (VBS) state [Fig. 7(a)] is the exact ground state of a certain extended Heisenberg Hamiltonian[10] and generally exhibits the properties inherent in the Haldane phase,[10,31,32,54] we can consider the state as an approximate ground state of the Heisenberg Hamiltonian. If we try to construct the VBS state on an open chain, the spin-S/2 degree of freedom is left unpaired at both the ends [Fig. 7(b)]. We are consequently led to the conclusion that the ground states of the spin-S open chain may be $(S+1)^2$-fold degenerate. The unpaired magnetic moment at each end is delocalized on the inner sites and weakly interact with each other in the real ground state.[7,8] It seems that the effective interaction between them is antiferromagnetic for even L's, while ferromagnetic for odd L's.[56] More explicitly, the quasidegenerate ground-state level structure of the spin-S open chain seems to be generally given as

$$(S_{\text{total}}=0)<(S_{\text{total}}=1)<\cdots<(S_{\text{total}}=S) \quad \text{for even } L\text{'s},$$

$$(S_{\text{total}}=S)<(S_{\text{total}}=S-1) <\cdots<(S_{\text{total}}=0) \quad \text{for odd } L\text{'s},$$

where S_{total} denotes the total spin of the state. In the $L\to\infty$ limit, the effective spin S/2's are decoupled and give the exactly $(S+1)^2$-fold degenerate ground state.

Now we are ready enough to discuss Fig. 6. Careful observation of Fig. 6 shows that the divergence is less sharp for even L's than for odd L's. However, the quantitative difference in the diverging behavior becomes less significant as L increases. They are all consistent with the above argument. In order to observe more explicitly the edge effect on the susceptibility, let us define the edge contribution χ_C as[16,17]

$$\chi_C=\chi_{L+1}^{\text{open}}-\chi_L^{\text{per}}, \tag{3.7}$$

where χ_L^{per} and χ_L^{open} are the susceptibilities of the L-sites periodic and open chains, respectively. Comparing Figs. 7(a) and 7(b), we find that the bulk contribution in χ_{L+1}^{open} should be identified with χ_L^{per} rather than χ_{L+1}^{per}. In Fig. 8 we show a temperature dependence of χ_C obtained through Eq. (3.7) with $L=96$. We have confirmed that all the data for $L=32$, 64, 96 give almost the same results for χ_C. We here observe that the numerical calculation of χ_C is well fitted by two curves according to temperature as

$$\frac{\chi_C J}{g^2\mu_B^2} = \begin{cases} \dfrac{4J}{3k_BT}=2\times\dfrac{1}{3}\left[\dfrac{S(S+1)J}{k_BT}\right]_{S=1} & \text{at low temperatures,} \\ \dfrac{2J}{k_BT}=\dfrac{1}{3}\left[\dfrac{S(S+1)J}{k_BT}\right]_{S=2} & \text{at high temperatures.} \end{cases} \tag{3.8}$$

Thus it turns out that the divergence at low temperatures is actually caused by the two edge moments with $S=1$, while the edge contribution at high temperatures is simply attributed to an $S=2$ free spin. There is also a transitional period between the above-mentioned temperature ranges, where the system is no more in the Haldane phase but a certain influence of the Haldane phase still remains. The fact that χ_C approaches the solid line from below suggests that the edge moment is an effective spin which is quantum-cooperatively constructed little by little with decrease of temperature. What we have observed here is a macroscopic evidence of a quantum-classical crossover in thermalization process and has been also found in the $S=1$ system.[57]

The high-temperature behavior of the susceptibility is given by a series-expansion method as

$$\chi_L=\frac{g^2\mu_B^2}{k_BT}\frac{\text{Tr}[(\Sigma_{i=1}^L S_i^z)^2 e^{-\beta\mathscr{H}}]}{\text{Tr}[e^{-\beta\mathscr{H}}]} = \begin{cases} \chi_\infty L\equiv\chi_L^{\text{per}} & \text{for the periodic chains,} \\ \chi_\infty L+\chi_0\equiv\chi_L^{\text{open}} & \text{for the open chains,} \end{cases} \tag{3.9}$$

where

$$\chi_\infty=\frac{g^2\mu_B^2}{J}\left(2\beta J-8(\beta J)^2+16(\beta J)^3\right)+O\left((\beta J)^4\right), \tag{3.10a}$$

$$\chi_0=\frac{g^2\mu_B^2}{J}\left(8(\beta J)^2-32(\beta J)^3\right)+O\left((\beta J)^4\right). \tag{3.10b}$$

Expression (3.10a) has been also shown in Fig. 6(a), which well fits the numerical data at $k_BT/J\gtrsim 6=[S(S+1)]_{S=2}$. Now an asymptotic behavior of χ_C is straightforwardly obtained as

$$\frac{\chi_C J}{g^2\mu_B^2}=2\beta J-16(\beta J)^3+O\left((\beta J)^4\right)\to 2\beta J\left(8(\beta J)^2\ll 1\right), \tag{3.11}$$

which is consistent with Eq. (3.8). If we represent the quantum-to-classical transitional period as $T_1<T<T_2$, k_BT_1 should be roughly identified with the Haldane gap Δ of the system, while T_2 may be given through Eq. (3.11) as $k_BT_2/J\simeq 2\sqrt{2}$, which is in good agreement with Fig. 8 and is also consistent with Fig. 4. It is to our interest to mention other integer-S cases. Representing the susceptibility of the L-site chain as Eq. (3.9), we obtain

$$\chi_\infty=\frac{g^2\mu_B^2}{J}\left(\frac{2}{3}\beta J-\frac{8}{9}(\beta J)^2+\frac{16}{27}(\beta J)^3\right)+O\left((\beta J)^4\right), \tag{3.12a}$$

$$\chi_0=\frac{g^2\mu_B^2}{J}\left(\frac{8}{9}(\beta J)^2-\frac{32}{27}(\beta J)^3\right)+O\left((\beta J)^4\right), \tag{3.12b}$$

for $S=1$ and

$$\chi_\infty=\frac{g^2\mu_B^2}{J}\left(4\beta J-32(\beta J)^2+128(\beta J)^3\right)+O\left((\beta J)^4\right), \tag{3.13a}$$

$$\chi_0=\frac{g^2\mu_B^2}{J}\left(32(\beta J)^2-256(\beta J)^3\right)+O\left((\beta J)^4\right), \tag{3.13b}$$

for $S=3$. Therefore, high-temperature behaviors of χ_C for $S=1$ and $S=3$ are, respectively, described as

$$\frac{\chi_C J}{g^2\mu_B^2}=\frac{2}{3}\beta J-\frac{16}{27}(\beta J)^3+O\left((\beta J)^4\right)\rightarrow\frac{2}{3}\beta J\quad\left(\frac{8}{9}(\beta J)^2\ll 1\right) \tag{3.14}$$

and

$$\frac{\chi_C J}{g^2\mu_B^2}=4\beta J-128(\beta J)^3+O\left((\beta J)^4\right)\rightarrow 4\beta J\quad\left(32(\beta J)^2\ll 1\right). \tag{3.15}$$

Here, $(2/3)\beta J$ in Eq. (3.14) and $4\beta J$ in Eq. (3.15) are to be regarded as $(1/3)[S(S+1)J/k_BT]_{S=1}$ and $(1/3)[S(S+1)J/k_BT]_{S=3}$, respectively. Now we obtain $k_BT_2/J\simeq 2\sqrt{2}/3$ for $S=1$ and $k_BT_2/J\simeq 4\sqrt{2}$ for $S=3$. The present discussion for $S=1$ is actually consistent with the numerical result.[57] It seems that while T_2 increases with S, $T_2/S(S+1)$ stays constant. A quantum-classical crossover of the same origin has been also observed in magnetization process of the $S=1$ system,[18] where the transitional field range is, as expected, given by $H_1<H<H_2$ with $g\mu_BH_1\simeq\Delta$ and $g\mu_BH_2\simeq k_BT_2$. As S increases, the Haldane gap rapidly goes to zero,[1] and the integer-S and half-odd-integer-S chains become less distinguishable. However, the influence of the quantum cooperation inherent in the Haldane phase remains far beyond the critical temperature (field), T_1 (H_1).

IV. SUMMARY

We have calculated thermodynamic quantities of $S=2$ antiferromagnetic Heisenberg chains under the periodic and open boundary conditions. The specific heat shows a well-pronounced Schottky anomaly at $k_BT/J\simeq 2$. However, we should note that the maximum is located at a temperature much larger than the Haldane gap, and the boundary condition, which affects the low-energy structure, has no significant effect on the temperature dependence. Therefore, in the present system, the temperature dependence of the specific heat should not be simply attributed to the energy gap between the ground state and the first excited state. It was unfortunate that the technical problem prevented us from observing the expected low-temperature behavior $C\propto e^{-\Delta/k_BT}$. On the other hand, the magnetic susceptibility strongly depends on the boundary condition. As $T\rightarrow 0$, the susceptibility vanishes for the periodic chains, while it diverges for the open chains. The edge contribution, which is obtained by subtracting the L-site periodic-chain susceptibility from the $(L+1)$-site open-chain one, is attributed to the two $S=1$ effective spins in the boundaries at low temperatures, while to an $S=2$ free spin at high temperatures. This is a visualization of a quantum-classical crossover in thermalization process and a strong evidence of the existence of the Haldane gap. It is rather difficult to extract an estimate of the $S=2$ Haldane gap from the present study. However, identifying the temperature T_1, below which the edge states are well formed, with Δ, we can roughly estimate the gaps for finite chains, $\Delta(L)$. They have been obtained as $\Delta(32)/J\sim 0.2$, $0.12\lesssim\Delta(64)/J\lesssim 0.14$, and $\Delta(96)/J\sim 0.1$ (see Fig. 8). These estimates are consistent with ones obtained through other methods.[35,39] Therefore we may at least conclude that the $S=2$ Haldane gap is smaller than $0.1J$. A more precise estimate of the $S=2$ Haldane gap will be presented elsewhere[39] through a quite different approach.

All the properties obtained here are also found in the $S=1$ case.[16,57] It has also turned out to be quite likely that all the arguments presented here are still valid for $S=3$. Now we may say that there are certain generic properties peculiar to the integer-S linear-chain quantum antiferromagnets. If we adopt an asymptotic formula[1] derived by Haldane,

$$\Delta\propto S(S+1)e^{-\pi\sqrt{S(S+1)}}, \tag{4.1}$$

together with the widely accepted numerical estimate[2,3] of the $S=1$ Haldane gap, $\Delta/J\simeq 0.4105$, we find three distinct temperature ranges as follows:

$T<T_1$: Haldane region,

$T_1<T<T_2$: quantum-to-classical transitional period,

$T_2<T$: classical region,

where

$$\frac{k_B T_1}{JS(S+1)} \simeq 0.2\times \exp[-\pi(\sqrt{S(S+1)}-\sqrt{2})], \tag{4.2a}$$

$$\frac{k_B T_2}{JS(S+1)} \simeq \frac{\sqrt{2}}{3}. \tag{4.2b}$$

There are also recent works[31,32] discussing a possibility that the Haldane phase for an arbitrary integer spin is characterized by a generic string order parameter.[9] The spectrum of low-lying states of the Haldane system may be in general explained by domain-wall excitations in the hidden order.[2,16,32] We hope that the present work will motivate further study on the $S>1$ Haldane systems not only in the theoretical field but also in the experimental one.

ACKNOWLEDGMENTS

The author would like to express his thanks to Professor S. Miyashita, Dr. M. Hagiwara, K. Totsuka, and Y. Nishiyama for stimulative discussions and useful comments. The author is also grateful to Y. Nishiyama for furnishing his unpublished numerical data. Numerical calculations were mainly carried out using the facilities of the Supercomputer Center, Institute for Solid State Physics, University of Tokyo. The present work is supported in part by a Grant-in-Aid from Ogasawara Foundation for the Promotion of Science & Engineering.

[1] F. D. M. Haldane, Phys. Lett. **93A**, 464 (1983); Phys. Rev. Lett. **50**, 1153 (1983).
[2] S. R. White and D. A. Huse, Phys. Rev. B **48**, 3844 (1993).
[3] O. Golinelli, Th. Jolicoeur, and R. Lacaze, Phys. Rev. B **50**, 3037 (1994).
[4] M. Takahashi, Phys. Rev. B **38**, 5188 (1988).
[5] K. Nomura, Phys. Rev. B **40**, 2421 (1989).
[6] S. Liang, Phys. Rev. Lett. **64**, 1597 (1990).
[7] S. R. White, Phys. Rev. Lett. **69**, 2863 (1992); Phys. Rev. B **48**, 10 345 (1993).
[8] S. Miyashita and S. Yamamoto, Phys. Rev. B **48**, 913 (1993).
[9] M. den Nijs and K. Rommelse, Phys. Rev. B **40**, 4709 (1989).
[10] I. Affleck, T. Kennedy, E. H. Lieb, and H. Tasaki, Phys. Rev. Lett. **59**, 799 (1987); Commun. Math. Phys. **115**, 477 (1988).
[11] J. P. Renard, M. Verdaguer, L. P. Regnault, W. A. C. Erkelens, J. Rossat-Mignod, and W. G. Stirling, Europhys. Lett. **3**, 945 (1987).
[12] K. Katsumata, H. Hori, T. Takeuchi, M. Date, A. Yamagishi, and J. P. Renard, Phys. Rev. Lett. **63**, 86 (1989).
[13] J. P. Renard, M. Verdaguer, L. P. Regnault, W. A. C. Erkelens, J. Rossat-Mignod, J. Ribas, W. G. Stirling, and C. Vettier, J. Appl. Phys. **63**, 3538 (1988).
[14] V. Gadet, M. Verdaguer, V. Briois, A. Gleizes, J. P. Renard, P. Beauvillain, C. Chappert, T. Goto, K. Le Dang, and P. Veillet, Phys. Rev. B **44**, 705 (1991).
[15] M. Orendáč, A. Orendáčová, J. Černák, A. Feher, P. J. C. Signore, M. W. Meisel, S. Merah, and M. Verdaguer, Phys. Rev. B **52**, 3435 (1995).
[16] S. Miyashita and S. Yamamoto, J. Phys. Soc. Jpn. **62**, 1459 (1993); S. Yamamoto and S. Miyashita, Phys. Rev. B **48**, 9528 (1993).
[17] S. Yamamoto and S. Miyashita, Phys. Rev. B **50**, 6277 (1994).
[18] S. Yamamoto and S. Miyashita, Phys. Rev. B **51**, 3649 (1995).
[19] C. Y. Weng, Ph.D. thesis, Carnegie Institute of Technology, 1968.
[20] H. W. J. Blöte, Physica B **79**, 427 (1975).
[21] C. S. Jain, K. Krishan, C. K. Majumdar, and V. Mubayi, Phys. Rev. B **12**, 5235 (1975).
[22] H. Betsuyaku and T. Yokota, Prog. Theor. Phys. **75**, 808 (1986).
[23] R. Narayanan and R. R. P. Singh, Phys. Rev. B **42**, 10 305 (1990).
[24] J. P. Renard, V. Gadet, L. P. Regnault, and M. Verdaguer, J. Magn. Magn. Mater. **90&91**, 213 (1990).
[25] M. Hagiwara, K. Katsumata, I. Affleck, B. I. Halperin, and J. P. Renard, Phys. Rev. Lett. **65**, 3181 (1990).
[26] O. Avenel, J. Xu, J. S. Xia, M-F. Xu, B. Andraka, T. Lang, P. L. Moyland, W. Ni, P. J. C. Signore, C. M. C. M. van Woerkens, E. D. Adams, G. G. Ihas, M. W. Meisel, S. E. Nagler, N. S. Sullivan, Y. Takano, D. R. Talham, T. Goto, and N. Fujiwara, Phys. Rev. B **46**, 8655 (1992).
[27] A. P. Ramirez, S.-W. Cheong, and M. L. Kaplan, Phys. Rev. Lett. **72**, 3108 (1994).
[28] H. Deguchi, S. Takagi, M. Ito, and K. Takeda, J. Phys. Soc. Jpn. **64**, 22 (1995).
[29] N. Fujiwara, J. R. Jeitler, C. Navas, M. M. Turnbull, T. Goto, and N. Hosoito, J. Magn. Magn. Mater. **140-144**, 1663 (1995).
[30] H. Kikuchi, Y. Ajiro, N. Mori, H. Aruga-Katori, T. Goto, and H. Nagasawa, Physica B **201**, 186 (1994); H. Kikuchi, H. Nagasawa, K. Mibu, T. Ono, N. Hosoito, and T. Shinjyo, J. Phys. Soc. Jpn. **64**, 3429 (1995).
[31] M. Oshikawa, J. Phys. Condens. Matter **4**, 7469 (1992).
[32] K. Totsuka and M. Suzuki, J. Phys. Condens. Matter **7**, 1639 (1995).
[33] Y. Hatsugai, J. Phys. Soc. Jpn. **61**, 3856 (1992).
[34] N. Hatano and M. Suzuki, J. Phys. Soc. Jpn. **62**, 1346 (1993).
[35] J. Deisz, M. Jarrell, and D. L. Cox, Phys. Rev. B **48**, 10 227 (1993).
[36] Y. Nishiyama, K. Totsuka, N. Hatano, and M. Suzuki, J. Phys. Soc. Jpn. **64**, 414 (1995).
[37] G. Sun, Phys. Rev. B **51**, 8370 (1995).
[38] U. Schollwöck and Th. Jolicœur, Europhys. Lett. **30**, 493 (1995).
[39] S. Yamamoto, Phys. Rev. Lett. **75**, 3348 (1995).
[40] C. Bellitto, L. P. Regnault, and J. P. Renard, J. Magn. Magn. Mater. **102**, 116 (1991).
[41] K. Katsumata, J. Magn. Magn. Mater. **140-144**, 1595 (1995); M. Hagiwara and K. Katsumata, *ibid.* **140-144**, 1665 (1995).
[42] M. Suzuki, in *Quantum Monte Carlo Methods*, edited by M. Suzuki (Springer-Verlag, Heidelberg, 1986), p. 2.
[43] J. E. Hirsch, R. L. Sugar, D. J. Scalapino, and R. Blankenbecler, Phys. Rev. B **26**, 5033 (1982).
[44] K. Binder and D. W. Heermann, in *Monte Carlo Simulation in Statistical Physics* (Springer-Verlag, Heidelberg, 1988), p. 5.
[45] H. Betsuyaku, Phys. Rev. Lett. **53**, 629 (1984); Prog. Theor. Phys. **73**, 319 (1985).
[46] M. Suzuki, Phys. Rev. B **31**, 2957 (1985).

[47] Y. Nishiyama, N. Hatano, and M. Suzuki (private communication).
[48] M. Suzuki, S. Miyashita, and A. Kuroda, Prog. Theor. Phys. **58**, 1377 (1977).
[49] R. Kubo, Phys. Rev. **87**, 568 (1952).
[50] H. Köhler and R. Schilling, J. Phys. Condens. Matter **4**, 7899 (1992).
[51] P. W. Anderson, Phys. Rev. **86**, 694 (1952).
[52] J. C. Bonner and M. E. Fisher, Phys. Rev. **135**, A640 (1964).
[53] D. P. Arovas, A. Auerbach, and F. D. M. Haldane, Phys. Rev. Lett. **60**, 531 (1988).
[54] I. Affleck, J. Phys. Condens. Matter **1**, 3047 (1989).
[55] T. Kennedy, J. Phys. Condens. Matter **2**, 5737 (1990).
[56] Y. Nishiyama (private communication).
[57] S. Yamamoto, J. Phys. Soc. Jpn. **64**, 4049 (1995).